PLANETARY SCIENCE

Deriving iron contents from past and future Venus surface spectra with new high-temperature laboratory emissivity data

J. Helbert[1]*, A. Maturilli[1], M. D. Dyar[2,3], G. Alemanno[1]

In situ information on the surface composition of Venus is based on measurements of a small number of landing sites. In the laboratory, we measured the emissivity of a range of igneous rocks at temperatures up to 480°C. We show that high-temperature laboratory spectra of basalts are consistent with the only existing multispectral data from the surface of Venus obtained by the photometers on the Venera 9 and 10 landers. We derive the FeO abundances for these landing sites of 12.2 and 9.5 weight %, respectively. From orbit, Venus' surface is only observable on the nightside through small spectral windows near 1 μm where the CO_2 atmosphere is largely transparent. The new laboratory data show that different rock types can be distinguished using only a small set of spectral bands. Therefore, future orbital spectral observations can provide a much-needed global composition map.

INTRODUCTION

Venus is the most Earth-like terrestrial planet in mass and radius in our solar system, yet little is known about its surface composition. The permanent cloud cover of Venus prohibits observation of the surface with traditional imaging techniques over most of the visible spectral range. Fortunately, Venus' CO_2 atmosphere is transparent in small spectral windows near 1 μm (*1*, *2*). Ground observers have successfully used these windows (*3*), as has the visible and infrared mapping spectrometer (VIMS) instrument on the Galileo mission on its way to Jupiter (*4*, *5*), the venus monitoring camera (VMC) and visible and infrared thermal imaging spectrometer (VIRTIS) instruments on the ESA Venus Express orbiter (*6*–*14*), and the Infrared 1 Micron (IR1) camera on the Japan Aerospace Exploration Agency (JAXA) Akatsuki orbiter (*15*). All these observations have revealed variations in surface brightness in these windows that are correlated with geological features (*9*, *11*), but the lack of applicable laboratory data for comparison has hampered compositional interpretations. Thus, our current understanding of Venus' surface depends mainly on the x-ray fluorescence instruments on the Soviet Venera 13 and 14 and Vega 2 landers, as well as Venera 8, 9, and 10 and Vega 1 and 2 gamma-ray spectrometers (*16*, *17*). The Venera 9 and 10 landers also carried photometers (*18*) that covered the visible to near-infrared (NIR) range (five broadband channels covering 0.45 to 1.1 μm), providing complementary data to the geochemical instruments. Multispectral data from the surface obtained by these landers allow us to verify that spectral data obtained from orbit can be used to derive compositional information from robust laboratory measurements under Venus conditions.

Understanding and interpreting visible and NIR spectra require spectral libraries acquired under conditions matching those on the surfaces being studied. Past and proposed measurements of the surface composition of Venus are hampered by the extreme surface conditions: ca. 470°C and 93 bars. Spectral shifts under Venus conditions result primarily from the high temperatures, which must be reproduced in the laboratory to provide appropriate calibration data. Venus surface pressure, on the other hand, has a negligible effect on the spectral features. For example, the dominant olivine absorption band at 1.04 to 1.08 μm (9615 to 9259 cm^{-1}) shifts ~130 cm^{-1}/GPa to lower wavelengths as pressure increases (*19*), which would be undetectable at Venus surface pressure of 93 bars (equal to 0.0093 GPa). Thus, effects of increased pressure on Venus surface spectra are comparatively benign as already noted by Pieters *et al.* (*20*).

In the last decade, the Planetary Spectroscopy Laboratory (PSL) of the Deutsches Zentrum von Luft- und Raumfahrt (DLR) in Berlin has provided spectral measurements of planetary analog materials at high temperatures from the mid- to far-infrared range (3 to 300 μm) for comparison with spacecraft data (*21*–*25*). From orbit, observations of the surface of Venus through the 1-μm windows can only be obtained on the nightside because reflected sunlight on the dayside swamps any surface contribution (*11*). Therefore, spectra of analog materials must be measured as emissivity, which is very challenging. In particular, thermal emission at these wavelengths is very low because it lies far below the main flank of the Planck curve for Venus surface temperatures, where the signal drops more than two orders of magnitude between 1.18 and 0.8 μm (see the "Experimental design" section). At the same time, many natural materials can be transparent at 1 μm. Mitigating these issues has required new protocols and highly sensitive equipment that have only recently been finalized (see the "Experimental design" section). At PSL, a combination of an InGaAs detector with matching Si on CaF_2 beam splitter, enhanced spectrometer electronics, and an optimized optical layout in the chamber (see the Experimental design section) is used to obtain these measurements.

Twelve natural rock samples were measured at 400°, 440°, and 480°C as a starting point for a database of Venus-analog materials (Table 1). They cover a range from felsic to mafic compositions (*5*, *17*, *26*) and cover all the expected grain sizes for Venus down to 250 μm: nine solid rock slabs and four powdered rock samples from 250 to 1000 μm. The preferred sample texture in this study was slabs rather than particulates because the Venus surface is not dominated by sediments, unlike other older solid bodies in our solar system such as Mars and Earth (*27*). Processes that transform coarse-grained blocks to loose material on Venus are far less efficient than on most other terrestrial planets. On Venus, surface wind speeds are quite slow (~1 m/s) (*28*), there is no water, and impact generation of a regolith by micrometeorites does not work in the constant way that

[1]DLR Berlin, Berlin, German. [2]Planetary Science Institute, 1700 East Fort Lowell, Suite 106, Tucson, AZ 85719, USA. [3]Department of Astronomy, Mount Holyoke College, 50 College St., South Hadley, MA 01075, USA.
*Corresponding author. Email: joern.helbert@dlr.de

Table 1. Rock samples studied and their composition.

	Hawaii alkali olivine basalt	Idaho Columbia River basalt	Lathrop Wells, NV trachybasalt	Kilauea fresh basaltic glass	Basalt Holyoke	Mount St. Helens andesite	Dacite Black Butte	Vinalhaven, Maine granite	Basalt Lake Yojoa, Honduras	Rhyolite Seiser Alm, Italy	Basalt Seiser Alm, Italy	Basalt Lanzarote Island, Spain
	Collection of M. McCanta, Univ. of Tennessee Knoxville	Collected for this project in Moscow, Idaho by M. Gunter, Univ. of Idaho	Collection of M. Rutherford, Brown University, sample LW-A	Collected by T. Orr, Hawaii Volcano Observatory	Collected in East Granby, CT from Lower Jurassic basalt in the Newark Supergroup, MA	Collection of M. McCanta, Univ. of Tennessee Knoxville	Collection of M. McCanta, Univ. of Tennessee Knoxville	Collection of S. Seaman, Univ. of Massachusetts Amherst	Collection of S. Mertzman, Franklin and Marshall College	Collections of University of Padua	Collections of University of Padua	Collections of University of Padua
	Slab	Slab	Slab	Powder: 700 to 1000 μm	Slab	Slab	Slab	Powder: 700 to 1000 μm	>500 μm; 250 to 500 μm	Slab	Slab	Slab
Na_2O	2.74	2.48	2.97	2.49	2.79	4.59	4.39	3.25	3.10	2.23	3.21	3.12
MgO	4.88	5.25	5.11	6.68	5.46	2.17	2.22	0.39	6.74	0.47	7.13	9.13
SiO_2	45.81	48.56	40.02	51.56	51.92	62.27	63.96	75.26	47.62	77.93	50.06	46.83
Al_2O_3	14.36	13.36	14.02	13.98	13.66	17.96	17.74	12.70	18.13	11.81	13.24	12.92
K_2O	0.88	1.15	1.52	0.44	0.70	1.23	1.14	5.00	1.06	5.29	2.45	1.04
CaO	10.09	8.96	16.05	10.93	9.33	5.41	5.53	0.89	10.11	0.17	8.89	10.51
TiO_2	2.14	3.11	1.72	2.50	1.04	0.66	0.45	0.30	2.04	0.08	0.95	2.99
MnO	0.18	0.30	0.16	0.17	0.21	0.08	0.06	0.07	0.16	0.01	0.22	0.17
FeO*	12.64	14.01	9.36	11.24	12.11	4.37	3.47	1.74	9.18	1.31	12.27	11.40
P_2O_5	0.29	0.78	1.10	0.24	0.13	0.14	0.15	0.07	0.45	0.01	0.30	0.53
Total	94.01	97.96	92.03	100.06	97.35	98.88	99.11	99.60	98.59	99.40	98.72	98.64

it does on airless (or near-airless) bodies. Even on Mars where chemical weathering was enabled by the presence of water, the existence of easily weathered minerals such as olivine requires that sediment production is primarily via physical processes (*29*). Although Mars has been impact gardened for billions of years, impact-generated sediments there have particle sizes >200 to 500 μm and aeolian-generated sediments create the finer grain sizes, <200 μm (*30*). Because wind erosion is inefficient on Venus, sediment sizes should largely mirror impact-generated particle sizes, i.e., >200 to 500 μm. Thus, our sample selection was biased toward selecting slabbed samples but included four particulate samples to cover the likely range of Venus sediment sizes.

Our new laboratory data can be used to interpret the decades-old Venera data. The Venera 9 and 10 descent modules carried identical photometers that measured light fluxes in five spectral ranges. The spectrometers were connected by fiber optics to optics placed above and below the aerobrake. Three optics separately collected radiation from the entire upper hemisphere, from the zenith, and from the lower hemisphere (*18*). After landing, the latter collected surface spectra that could be calibrated using the down-welling radiation measured from the upper hemisphere (*31*). These are the only existing multispectral measurements from the surface of Venus. Those data from figure 8 of Ekonomov *et al.* (*18*) were digitized (see Materials and Methods) and converted to emissivity using the Kirchhoff's law. The photometer had broadband channels, and we follow here the assignment of the central wavelength based on the instrument transfer function by Avduevskii *et al.* (*31*) and improved by Ekonomov *et al.* (*18*). For context, the inset in Fig. 1 shows images of the landing sites of Venera 9 and 10 obtained by the Panoramic Telephotometer, while the photometers acquired their measurements from the opposite side of the lander. Ekonomov *et al.* (*18*) found that the Venus

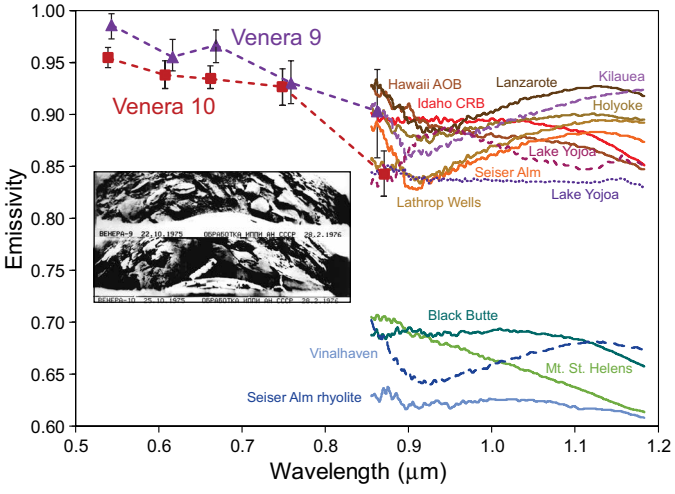

Fig. 1. Laboratory emissivity data obtained at 440°C sample temperature (solid lines) compared to multispectral data from the Venera 9 and 10 landers [reflectance converted to emissivity with associated error bars digitized from figure 8 of Ekonomov *et al.* (*18*)]. Dashed lines indicate particles with ranges of grain sizes: 700 to 1000 μm (long dashes), >500 μm (medium dash), and 250 to 500 μm (dots). This is the first direct spectral confirmation that Venera 9 and 10 landed on basaltic material. The inset shows images of the landing site obtained by the Panoramic Telephotometer [Venera 9–NASA Space Science Data Coordinated Archive (NSSDC) dataset ID (photo): 75-050D-01A; Venera 10–NSSDC dataset ID (photo): 75-054D-01A]. The spectra were obtained in both cases on the opposite side of the lander.

soil and some kinds of basalts measured at room temperatures have very similar values of albedo. However, the slopes longward of 0.8 μm were very different [see figures 11 and 12 of Ekonomov *et al.* (*18*)]. In (*18*) the word "soil" is used to generally describe the surface material of Venus, not in the sense as it is used by geologists; see Materials and Methods.

RESULTS

Figure 1 compares ground truth data from the Venera landers to our recent laboratory measurements. Laboratory spectra obtained at Venus surface temperature for basaltic rock types match the one overlapping wavelength band of the in situ data in absolute emissivity. Previous interpretations of the composition were solely based on the measured thorium and uranium content and its comparison to terrestrial analogs (*32*). To check on the influence of particle size versus slabs, we included four particulate igneous samples: Maine granite and fresh Hawaiian basaltic glass (700 to 1000 μm) and two size fractions of a Honduran basalt (250 to 500 μm and >500 μm). In no case did the particulate spectra vary more than slightly from the slab spectra of compositionally similar samples, indicating that to first order, composition and not grain size is the dominating factor. Further work is in progress to evaluate this effect more systematically.

Additional information can be extracted from the laboratory data by considering the relationship between the FeO contents of the rocks studied and NIR emissivity that might be detected from space (*33*). The atmosphere of Venus has five spectral windows between 0.86 and 1.18 μm with varying width and transparency (*17*). Since VIMS on Galileo (*34*) and VIRTIS on Venus Express (*8*, *11*, *17*) reported surface emissivity variations, there has been discussion of how much compositional information can be derived from those five spectral windows. Neither instrument was designed to observe the surface of Venus. Building on experience from Venus Express, new instrument concepts have been designed specifically to use those atmospheric windows to map the surface composition of Venus. For example, the Venus Emissivity Mapper (VEM) is part of the payload of several proposed Venus missions (*35*–*37*). It uses six spectral bands to map the surface within the five available windows. To assess how useful data from such an instrument on an orbiter or an aerial platform might be to derive surface composition, we have convolved the spectra with the transfer function for each filter in the VEM instrument following the band shape of each atmospheric window (the 1.02-μm window being sampled by two filters). The resulting six-point spectra are shown in Fig. 2.

An instrument like VEM (*36*, *37*) could achieve an uncertainty in emissivity retrieval of 0.9% using state-of-the-art radiative transfer models to correct for atmospheric influences and with an improved Venus surface topography (see Materials and Methods). To be conservative, we assume, for our comparison here, an uncertainty of 4%. Even with this uncertainty, the distinction between mafic, felsic, and intermediate materials is clearly possible.

Emissivity varies with total transition metal content of the samples, but the biggest contributor to the signal is crystal field transitions arising from Fe. So, calibrated laboratory emissivities at each of the six bands for the 13 samples were regressed using partial least squares against weight % (wt %) FeO_{total}. The resultant relationship allows prediction of wt % FeO with a root mean squared error of ±0.72 (in units of wt % FeO_{total}) based on 13-fold (leave-one-out) cross-validation (LOO-CV) (see the "Statistical analysis" section). These error

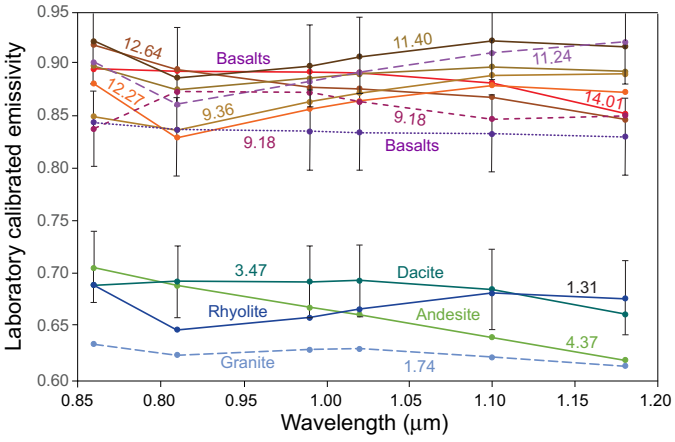

Fig. 2. Emissivity data from Fig. 1 down-sampled to the filters used by the VEM (*36*). The five spectral windows between 0.86 and 1.18 μm in the atmosphere of Venus are mapped with six filters (the 1.02-μm window being sampled by two filters). Numbers indicate wt % FeO and dashed lines indicate particles with ranges of grain sizes: 700 to 1000 μm (long dashes), >500 μm (medium dash), and 250 to 500 μm (dots). Error bars added to select samples represent a conservative assumption on the uncertainty of ±4% for the retrieval of emissivity from orbit including instrumental and atmospheric effects and show that variations in rock composition can be determined from orbit. Errors on laboratory measurements are smaller than symbols.

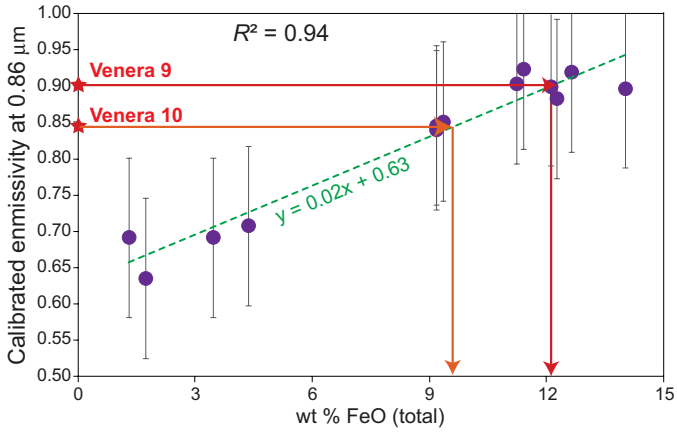

Fig. 3. Total Fe expressed as wt % FeO of the igneous samples shows a correlation with the calibrated emissivity at 0.86 μm. Error bars represent leave-one-out cross-validation (LOO-CV) for linear regression. FeO contents to be derived for the Venera 9 and 10 landing sites based on their spectral measurements [reflectance converted to emissivity with associated error bars digitized from figure 8 of Ekonomov *et al.* (*19*): $\varepsilon_{Venera9}$ is ±0.04 and $\varepsilon_{Venera10}$ is ±0.02]. On the basis of this analysis, Venera 9 has 12.2 wt % FeO_{total} and Venera 10 has 9.5 wt % FeO_{total}. XRF, x-ray fluorescence.

bars are much smaller than the difference in FeO content between basalt (~7 to 13 wt % in this dataset) and granite (ca. 0 to 2 wt %). These results show that orbital observations can provide a much-needed global map of surface composition on the basis of FeO contents, enabling a deeper understanding of the evolution of Venus as a terrestrial planet and as an analog for Earth-sized exoplanets. We expect to use this method to continually improve this expression as new data are added to the database.

Moreover, our new data can be used to derive iron contents from Venera 9 and 10 photometer data in the absence of an x-ray fluorescence instrument. Figure 3 relates intensity at 0.86 μm and FeO_{total} for samples studied. Overplotted are converted emissivity interpolated to 0.86 μm from Venera 9 and 10 data. The correlation between band wavelength and FeO content suggests that the Venera 9 landing site can be inferred to have 12.2 ± 2 and 9.5 ± 1 wt % for Venera 10. These are the first quantitative determinations of the FeO abundance for these two landing sites and are comparable with total FeO measured by x-ray fluorescence at Vega 2 (7.7 ± 1.1 wt %), Venera 13 (9.4 ± 2.2 wt %), and Venera 14 (9.0 ± 1.18 wt %) (*38*). Photogeologic analysis (*16*) of Venera 9 and 10 landing sites further indicates plains with wrinkle ridges. These several lines of evidence all point to volcanic plains material.

DISCUSSION

Figure 1 shows calibrated emissivity at 440°C in full spectrometer resolution. Improving upon preliminary results presented earlier (*39*), these data show substantially increased spectral contrast between rock types. This improvement results from careful alignment of the optical pathway and changes in the shape of the ceramic sample enclosure. The comparison of in situ spectra obtained by the Venera 9 and 10 with the high-temperature laboratory data shows a match between the two datasets in absolute emissivity. Absolute emissivity values are not commonly used in remote sensing analysis but are required here, given the single data point of overlap between the Venera spectra and laboratory spectra.

Some workers have proposed that a hematite-rich coating should form almost instantly under Venus-like conditions (*40*), but they are based on experiments conducted under mismatched conditions (600° to 900°C in air) not directly applicable to Venus. However, kinetics and breakdown reactions of basalt under more realistic Venus conditions (*41*) indicate diffusion of Ca > Fe > Mg toward the Venus atmosphere, resulting in anhydrite coatings. These results are supported by recent experiments using true Venus surface temperatures (*42*, *43*), indicating that thin (~6 μm/100,000 years) coatings on Venus rocks are a mixture of spectrally transparent sulfate (anhydrite) and metastable carbonate with dispersed submicrometer oxide (*41*). At NIR wavelength, this coating should not affect the spectra (*41*), which is confirmed by the match between the Venera 9 and 10 spectra and the laboratory spectra of nonweathered basalt.

Figure 2 shows that even reducing the spectral resolution to only the atmospheric windows in the atmosphere of Venus still allows meaningful insights into surface composition to be derived. For example, more Fe/Mg-rich mafic materials (here, basalts) show higher emissivities (regardless of whether they are particulate or slabs) than Si-rich felsic materials (again, whether particulate or slab) by almost 30%. This is consistent with early suggestions (*5*) based on Galileo NIMS data and observations from the VIRTIS instrument on Venus Express (*8*, *34*) that favor a felsic composition for low-emissivity tesserae on Venus. Tessera plateaus are proposed equivalents of Earth's continents, which may require basalt to be melted in the presence of water to form. An essential question for the evolution of Venus is whether or not tessera terrains are felsic in composition. Tesserae occur in huge plateaus covering 7% of the surface and represent a volume too large to be a result of anhydrous fractional crystallization. A key question for understanding the history of water and habitability on Venus is thus whether or not tesserae are equivalent to Earth's continents and thus formed in the presence of water (*44*). A deep understanding of planetary habitability requires identifying

the key factors that govern the environment over time. Venus is the ultimate control case for understanding how Earth developed and maintained conditions suited to life. Tesserae are key here because they are a window into a past period of Venus.

Figure 3 shows that FeO content is one of the dominating factors in this spectral range. To predict the FeO content of the Venera landing sites, we derive a relation between emissivity in the 0.86-μm band and the FeO content, which can be continually improved as new data are added to the database. Exploiting this relation, we derived an FeO content for the rocks at the Venera 9 and 10 landing sites. Other data from the Venus landers lend further insight into the type of basalts that may be present. Gamma-ray spectrometers for K, U, and Th rock analyses were carried on Vega 1 and 2 as well as Venera 8, 9, and 10. The Venera 10 landing site has relatively low K, U, and Th contents, implying an origin from a more depleted (of incompatible elements) source. Low abundances of these incompatible elements ($\frac{\text{Concentration}_{\text{mineral}}}{\text{Concentration}_{\text{melt}}} < 1$) have been interpreted to originate from a mantle source region that has repeatedly melted; melt leaves to form the Venus crust. Concentrations may also be diluted by high degrees of partial melting. Conversely, source regions that have had less melt extracted or smaller degrees of partial melting have higher K, U, and Th values, as observed by Venera 9.

On Earth, Hawaiian basalts are interpreted to result from plumes sourced from a less depleted mantle source region, and their incompatible elements vary with differences in partial melting. In Fig. 2, Venera 9 total FeO overlaps with Hawaiian alkali olivine basalt, thought to derive from lower degrees of partial melting resulting in high incompatible element concentrations. Venera 10 total FeO results overlap with those from fresh Kilauea tholeiitic basalts that represent higher degrees of partial melting and diluting and therefore lower the overall concentration of the incompatible elements. While not unambiguous, the new FeO data and the Venera gamma-ray spectrometer data are complementary and support previous ideas for the geochemistry of the Beta Regio area (*16*).

The work presented here shows that future orbital observations could provide a much-needed global map of surface composition on the basis of FeO contents. As can be seen from our comparison with Venera 9 and 10 data, the orbital observations can be linked directly to observations obtained by landers and future aerial platforms. Combined together, these data will enable a deeper understanding of the evolution of Venus as a terrestrial planet and as an analog for Earth-sized exoplanets.

MATERIALS AND METHODS

Samples studied and methods

Samples studied are summarized in Table 1. They are part of collections at the Mount Holyoke College and the PSL at DLR. The samples were also chosen on the basis of availability of samples large enough to prepare a 5-cm-diameter, 4-mm-thick round disk suitable for the sample holder in the experiments. The disks were prepared from the sample interior by cutting a square chip with dimensions of 5 cm by 5 cm and then rounding the corners by hand on a grinding wheel. For Kilauea fresh basaltic glass, Vinalhaven (Maine) granite, and Lake Yojoa (Honduras) basalt, samples were run as particulates with grain sizes of 700 of 1000 μm for glass and granite and of 500 to 1000 μm and 250 to 500 μm for the Honduran basalt.

Separate small aliquots of each sample were ground for 10 s in a tungsten shatterbox and sieved to grain sizes of less than 63 μm for compositional analysis. Compositions given in Table 1 of the text were determined by X-Ray Fluorescence Bureau Veritas Commodities Canada Ltd. using their LF302 package.

Venera 9 and 10 data

To obtain values for the emissivity from the Venera 9 and 10 photometer reflectance measurements, figure 8 of Ekonomov *et al.* (*18*) was digitized using https://automeris.io/WebPlotDigitizer. The resulting values were converted to emissivity applying Kirchhoff's law ($\varepsilon = 1 - R$). Venera 9 and 10 used broadband photometers. Assignment of the central wavelength used here follows the updated determination by Ekonomov *et al.* (*18*).

Ekonomov *et al.* used in (*18*) the word soil to generally describe the surface material of Venus as can be seen in equation 3. This is even more obvious on page 72 where they state that "While estimating the composition of Martian rocks by the spectrum of their reflection, it was determined that the albedo of the Mars soil can be fitted by the mixture of various rocks, for example, basalt + goethite; basalt + limonite." The word soil is not used as it would be by a geologist or, perhaps, is mistranslated.

The Venera 9 landing area is situated between the northeast part of Beta Regio and the northern part of Hyndla Regio on the extension of the northeast branch of the Devana Chasma, the axial rift of Beta Regio (*16*). The center of the landing site ellipse is 900 km to the east of Rhea Mons, in the region of Aikhylu Chasma, at 31.01°N, 291.64°E. The radius of the landing site ellipse (circle) is ~150 km. The photogeologic analysis (*16*) shows that the material of plains with wrinkle ridges dominates the Venera 9 landing site ellipse (it occupies ~60% of the area of the ellipse). The material of plains with fractures and ridges and the material of tesserae occupy ~21 and ~14% of the area of the landing site ellipse, respectively. The remaining area of the ellipse (~4%) is occupied by the material of shield plains. The Venera 10 landing area is located in the southern part of Hyndla Regio, to the southeast of Beta Regio, 800 km to the east of the axial rift Devana Chasma. The landing site ellipse is centered at 15.42°N, 291.51°E (*16*). The radius of the landing site ellipse (circle) is ~150 km. Photogeologic analysis (*16*) has shown that the ellipse of the Venera 10 landing site region is dominated by the material of plains with

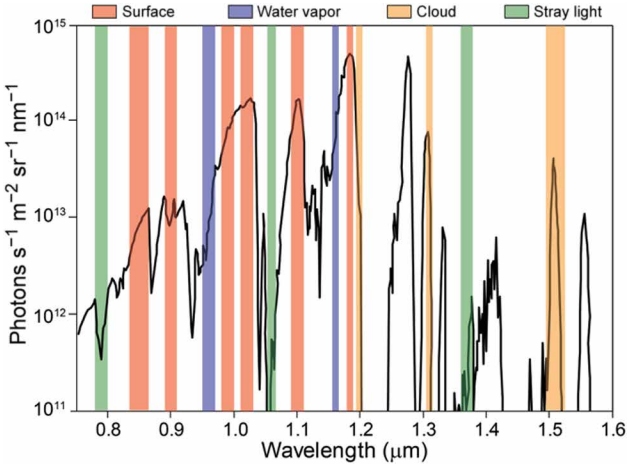

Fig. 4. Wavelengths of bands used opportunistically around gaps in the CO_2 atmosphere of Venus (*54*). Collectively, these offer a comprehensive sampling of surface, water vapor cloud opacity, and stray light, as needed to estimate errors on surface bands. The black line is an observed nightside emission spectrum of Venus.

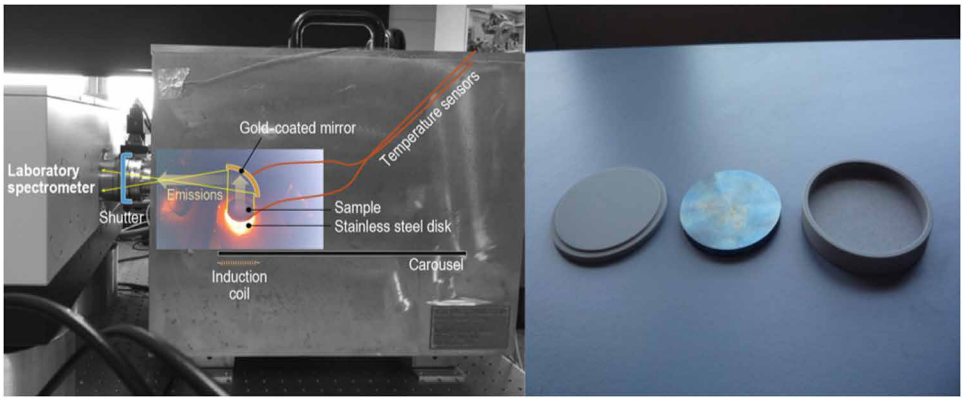

Fig. 5. Venus high-temperature spectroscopy setup at PSL. (**Left**) Unique high-temperature chamber at PSL with induction heating system optimized for emissivity measurements in the 1-μm region. (**Right**) Ceramic enclosure used for Venus measurements to suppress thermal radiation from the hot steel that would reflect of the sample drowning out the emissivity signal. Photo credit: Jörn Helbert, DLR.

wrinkle ridges, which occupies ~60% of the ellipse area. The material of lobate plains and the material of tesserae occupy ~21% and ~15% of this area, respectively. The remaining 4% of the ellipse area is embayed by the unit of densely fractured plains, the unit of plains with fractures and ridges, and the unit of shield plains.

Atmospheric uncertainties

Processing of radiance data to emissivity requires not only quantification of these atmospheric effects but also information about surface temperature, elevation, and instrument calibration. This atmospheric correction technique for the transparent windows in the atmosphere of Venus around 1 μm (Fig. 4) and expected uncertainties from the instrument and topography uncertainties for a VEM-like instrument have been discussed in (*36*, *45*) as an update of the work in (*10*, *46*, *47*) for VIRTIS on Venus Express. The analysis shows that a VEM-like instrument can achieve an uncertainty in the surface emissivity retrieval of significantly less than 4%.

Experimental design

The PSL high-temperature chamber (Fig. 5) is attached to a Bruker Vertex 80v Fourier Transform Spectrometer that allows heating of samples to temperatures up to 1000 K under vacuum conditions (medium vacuum ≈ 10 to 100 Pa) (*25*). Samples are placed in steel cups equipped with type K thermocouples as temperature sensors. A copper induction coil installed in the chamber and connected to a Linn High Therm 1.5-kW induction system allows contactless heating of ferromagnetic sample cups by induction. This system has been used successfully for many years to study the effect of temperature on the NIR to mid-infrared spectra for Mercury (*21*–*24*).

The setup at PSL focuses on obtaining high signal-to-noise measurements. The low emissivity signal of the sample versus the emissivity of the stainless steel used for the sample cup (especially toward shorter wavelength at high temperatures) resulted in a non-negligible contribution to the total radiance from sample cups. After extensive testing, a ceramic enclosure was built to embed the steel disk needed to heat the samples. This reduced the contribution coming from the glowing steel. Figure 5 shows the ceramic enclosure and the steel disk that we use to embed inside. This ceramic enclosure is made of FRIALIT GP79 (Si_3N_4), with a low emissivity in the visible spectral range.

Spectra were measured under vacuum with the Bruker Vertex 80v spectrometer equipped with an InGaAs detector and a Si on CaF_2 beam splitter. The samples were heated under vacuum to 480°C. The signal-to-noise ratio [root mean square (RMS)] on a single measurement with 500 scans for a sample at 400°C determined with the Bruker OPUS software during the measurement was greater than 10 in all cases. Sample temperature is monitored by a thermocouple (accuracy, <0.1 K) in direct contact with the emitting surface. Repeating the assessment from (*48*) at high temperatures, the relative error (two measurements on the sample at the same temperature measured by the thermocouple) in % is less than 0.0005. After the sample measurements, a blackbody sample (an electro-furnace slag slab with same dimensions as the samples) was measured at the same temperature and under the same conditions (heating in the same sample cup, monitored with the same thermocouple). The emissivity curve of the blackbody sample is derived from inverting its hemispherical reflectance measurement. The high-temperature blackbody sample is regularly measured against a Polytec SR 800 calibration blackbody that is regularly calibrated by the Physikalisch-Technische

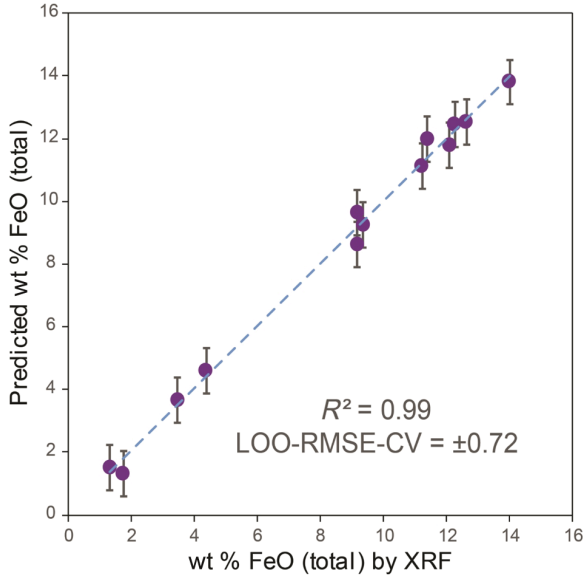

Fig. 6. Results of six-channel partial least squares model regressing calibrated intensity at each channel against total wt % FeO using all standards in Table 1. Error bars are solely prediction errors.

Bundesanstalt (https://www.ptb.de/cms/en.html), the German federal calibration authority (*49*). Emissivity was derived as the ratio between the sample radiance and the blackbody radiance multiplied by the known emissivity curve of the high-temperature blackbody, following the same approach as used by the Physikalisch-Technische Bundesanstalt for high-temperature emissivity measurements of materials (*25*, *48*–*50*).

Statistical analysis

Prediction of total FeO was here undertaken using partial least squares analysis (PLS, 40) (*51*) using a web tool that uses the scikit-learn library (*52*). PLS was developed for use in situations where highly collinear explanatory (p) variables significantly outnumber observations (N), such that $p >> N$ (*53*). Model accuracy was evaluated using leave-one-out cross-validation (LOO-CV) to obtain RMS errors (RMSE). LOO-RMSE-CVs are similar to simple calibration errors, except that one sample is removed from the training set, a model is made from the remaining $n - 1$ samples, and the prediction error for the withheld sample is found. This process is done iteratively over all samples to make n "folds" (Fig. 6).

REFERENCES AND NOTES

1. D. A. Allen, J. W. Crawford, Cloud structure on the dark side of Venus. *Nature* **307**, 222–224 (1984).
2. J. B. Pollack, J. B. Dalton, D. Grinspoon, R. B. Wattson, R. Freedman, D. Crisp, D. A. Allen, B. Bezard, C. DeBergh, L. P. Giver, Q. Ma, R. Tipping, Near-infrared light from Venus' nightside: A spectroscopic analysis. *Icarus* **103**, 1–42 (1993).
3. V. S. Meadows, D. Crisp, Ground-based NIR observatiosn of Venus nightside: The thermal structure and water abundance near the surface. *J. Geophys. Res.* **101**, 4595–4622 (1996).
4. K. H. Baines, S. Atreya, R. W. Carlson, D. Crisp, P. Drossart, V. Formisano, S. S. Limaye, W. J. Markiewicz, G. Piccioni, To the depths of Venus: Exploring the deep atmosphere and surface of our sister world with Venus Express. *Planet. Space Sci.* **54**, 1263–1278 (2006).
5. G. L. Hashimoto, S. Sugita, On observing the compositional variability of the surface of Venus using nightside near-infrared thermal radiation. *J. Geophys. Res.* **108**, 5109 (2003).
6. A. T. Basilevsky, E. V. Shalygin, D. V. Titov, W. J. Markiewicz, F. Scholten, T. Roatsch, M. A. Kreslavsky, L. V. Moroz, N. I. Ignatiev, B. Fiethe, B. Osterloh, H. Michalik, Geologic interpretation of the near-infrared images of the surface taken by the Venus Monitoring Camera, Venus Express. *Icarus* **217**, 434–450 (2012).
7. P. D'Incecco, N. Müller, J. Helbert, M. D'Amore, Idunn Mons on Venus: Location and extent of recently active lava flows. *Planet. Space Sci.* **136**, 25–33 (2017).
8. M. S. Gilmore, N. Mueller, J. Helbert, VIRTIS emissivity of Alpha Regio, Venus, with implications for tessera composition. *Icarus* **254**, 350–361 (2015).
9. J. Helbert, N. Müller, P. Kostama, L. Marinangeli, G. Piccioni, P. Drossart, Surface brightness variations seen by VIRTIS on Venus Express and implications for the evolution of the Lada Terra region, Venus. *Geophys. Res. Lett.* **35**, L11201 (2008).
10. D. Kappel, G. Arnold, R. Haus, Multi–spectrum retrieval of Venus IR surface emissivity maps from VIRTIS/VEX nightside measurements at Themis Regio. *Icarus* **265**, 42–62 (2016).
11. N. Mueller, J. Helbert, G. L. Hashimoto, C. C. C. Tsang, S. Erard, G. Piccioni, P. Drossart, Venus surface thermal emission at 1μm in VIRTIS imaging observations: Evidence for variation of crust and mantle differentiation conditions. *J. Geophys. Res.* **113**, (2008).
12. N. T. Mueller, S. E. Smrekar, C. C. C. Tsang, Multispectral surface emissivity from VIRTIS on Venus Express. *Icarus* **335**, 113400 (2020).
13. S. E. Smrekar, E. R. Stofan, N. Mueller, A. Treiman, L. Elkins-Tanton, J. Helbert, G. Piccioni, P. Drossart, Recent hotspot volcanism on Venus from VIRTIS emissivity data. *Science* **328**, 605–608 (2010).
14. E. R. Stofan, S. E. Smrekar, N. Mueller, J. Helbert, Themis Regio, Venus: Evidence for recent (?) volcanism from VIRTIS data. *Icarus* **271**, 375–386 (2016).
15. M. Nakamura, T. Imamura, N. Ishii, T. Abe, Y. Kawakatsu, C. Hirose, T. Satoh, M. Suzuki, M. Ueno, A. Yamazaki, N. Iwagami, S. Watanabe, M. Taguchi, T. Fukuhara, Y. Takahashi, M. Yamada, M. Imai, S. Ohtsuki, K. Uemizu, G. L. Hashimoto, M. Takagi, Y. Matsuda, K. Ogohara, N. Sato, Y. Kasaba, T. Kouyama, N. Hirata, R. Nakamura, Y. Yamamoto, T. Horinouchi, M. Yamamoto, Y. Y. Hayashi, H. Kashimura, K. I. Sugiyama, T. Sakanoi, H. Ando, S. Y. Murakami, T. M. Sato, S. Takagi, K. Nakajima, J. Peralta, Y. J. Lee, J. Nakatsuka, T. Ichikawa, K. Inoue, T. Toda, H. Toyota, S. Tachikawa, S. Narita, T. Hayashiyama, A. Hasegawa, Y. Kamata, AKATSUKI returns to Venus. *Earth Planets Space* **68**, 75 (2016).
16. A. M. Abdrakhimov, A. T. Basilevsky, Geology of the venera and vega landing-site regions. *Solar Syst. Res.* **36**, 136–159 (2002).
17. M. Gilmore, A. Treiman, J. Helbert, S. Smrekar, Venus surface composition constrained by observation and experiment. *Space Sci. Rev.* **212**, 1511–1540 (2017).
18. A. P. Ekonomov, Y. M. Golovin, B. E. Moshkin, Visible radiation observed near the surface of Venus: Results and their interpretation. *Icarus* **41**, 65–75 (1980).
19. T. J. Shankland, A. G. Duba, A. Woronow, Pressure shifts of optical absorption bands in iron-bearing garnet, spinel, olivine, pyroxene, and periclase. *J. Geophys. Res.* **79**, 3273–3282 (1974).
20. C. M. Pieters, J. W. Head, S. Pratt, W. Patterson, J. Garvin, V. L. Barsukov, A. T. Basilevsky, I. L. Khodakovsky, A. S. Selivanov, A. S. Panfilov, Y. M. Gektin, Y. M. Narayeva, The color of the surface of Venus. *Science* **234**, 1379–1383 (1986).
21. S. Ferrari, F. Nestola, M. Massironi, A. Maturilli, J. Helbert, M. Alvaro, M. C. Domeneghetti, F. Zorzi, In-situ high-temperature emissivity spectra and thermal expansion of C2/c pyroxenes: Implications for the surface of Mercury. *Am. Mineral.* **99**, 786–792 (2014).
22. J. Helbert, A. Maturilli, The emissivity of a fine-grained labradorite sample at typical Mercury dayside temperatures. *Earth Planet. Sci. Lett.* **285**, 347–354 (2009).
23. J. Helbert, A. Maturilli, M. D'Amore, Visible and near-infrared reflectance spectra of thermally processed synthetic sulfides as a potential analog for the hollow forming materials on Mercury. *Earth Planet. Sci. Lett.* **369**, 233–238 (2013).
24. J. Helbert, F. Nestola, S. Ferrari, A. Maturilli, M. Massironi, G. J. Redhammer, M. T. Capria, C. Carli, F. Capaccioni, M. Bruno, Olivine thermal emissivity under extreme temperature ranges: Implication for Mercury surface. *Earth Planet. Sci. Lett.* **371**, 252–257 (2013).
25. A. Maturilli, J. Helbert, G. Arnold, M. Strojnik, G. E. Arnold, The newly improved set-up at the Planetary Spectroscopy Laboratory (PSL) The newly improved set-up at the Planetary Spectroscopy Laboratory (PSL), paper presented at the Infrared Remote Sensing and Instrumentation XXVII, 9 September 2019.
26. M. Zolozov, Gas–solid interactions on Venus and other solar system bodies. *Rev. Mineral. Geochem.* **84**, 351–392 (2018).
27. C. M. Weitz, J. J. Plaut, R. Greeley, R. S. Saunders, Dunes and microdunes on Venus: Why were so few found in the Magellan data? *Icarus* **112**, 282–295 (1994).
28. R. D. Lorenz, Surface winds on Venus: Probability distribution from in-situ measurements. *Icarus* **264**, 311–315 (2016).
29. M. Golombek, C. Charalambous, W. T. Pike, R. Sullivan, The Origin of Sand and Dust on Mars: Evidence from the Insight Landing Site, paper presented at the 51st Lunar and Planetary Science Conference, 2020, #2744.
30. M. Golombek, C. Charalambous, W. T. Pike, R. Sullivan, Relative Magnituedes of Water Sources to the Lunar Poles, paper presented at the 51st Lunar and Planetary Science Conference, 2018, #2319.
31. V. S. Avduevskii, Y. M. Golovin, F. S. Zavelevich, V. Y. Likhushin, M. Y. Marov, D. A. Melnikov, Y. I. Merson, B. E. Moshkin, K. A. Razin, L. I. Chernoshchekov, A. P. Èkonomov, Preliminary results of the direct measurements of radiation fluxes from the Sun in the atmosphere and at the surface of Venus, conducted aboard the descent modules of the "Venera-9" and "Venera-10" automatic interplanetary stations. *Dokl. Akad. Nauk SSSR* **229**, 579–582 (1976).
32. Y. A. Surkov, Studies of Venus rocks by Veneras 8, 9 and 10, in *Venus,* D. M. Hunten, L. Colin, T. M. Donahue, V. I. Moroz, Eds. (University of Arizona Press, 1983), pp. 154–158.
33. M. D. Dyar, J. Helbert, A. Maturilli, N. T. Müeller, D. Kappel, Probing Venus surface iron contents with six-band visible near-infrared spectroscopy from orbit. *Geophys. Res. Lett.* **47**, e2020GL090497 (2020).
34. G. L. Hashimoto, M. Roos-Serote, S. Sugita, M. S. Gilmore, L. W. Kamp, R. W. Carlson, K. H. Baines, Felsic highland crust on Venus suggested by Galileo near-infrared mapping spectrometer data. *J. Geophys. Res.* **113**, E00B24 (2008).
35. R. C. Ghail, C. Wilson, M. Galand, D. Hall, C. Cochrane, P. Mason, J. Helbert, F. MontMessin, S. Limaye, M. Patel, N. Bowles, D. Stam, J. E. Wahlund, F. Rocca, D. Waltham, T. A. Mather, J. Biggs, M. Genge, P. Paillou, K. Mitchell, L. Wilson, U. N. Singh, EnVision: Taking the pulse of our twin planet. *Exp. Astron.* **33**, 337–363 (2012).
36. J. Helbert, A. Maturilli, M. D'Amore, I. Varatharajan, Y. R. Ortiz, The Planetary Spectroscopy Laboratory (PSL): wide spectral range, wider sample temperature range, in *Infrared Remote Sensing and Instrumentation XXVI* (SPIE, 2018), vol. 10765.
37. J. Helbert, A. C. Vandaele, E. Marq, S. Robert, C. Ryan, G. Guignan, Y. Rosas-Ortiz, E. Neefs, I. R. Thomas, G. Arnold, G. Peter, T. Widemann, L. Laray, The VenSpec suite on the ESA EnVision mission to Venus, *Infrared Remote Sensing and Instrumentation XXVII* (9 September 2019).
38. J. S. Kargel, G. Komatsu, V. R. Baker, R. G. Storm, The volcanology of venera and VEGA landing sites and the geochemistry of Venus. *Icarus* **103**, 253–275 (1993).
39. J. Helbert, A. Maturilli, M. D. Dtarm S. Ferrari, N. Müller, S. Smrekar, Orbital Spectroscopy of the Surface of Venus, paper presented at the 49th Lunar and Planetary Science Conference, 01 March 2018, #1219.

40. J. Filiberto, D. Trang, A. H. Treiman, M. S. Gilmore, Present-day volcanism on Venus as evidenced from weathering rates of olivine. *Sci. Adv.* **6**, eaax7445 (2020).
41. M. D. Dyar, J. Helbert, R. F. Cooper, E. C. Sklute, A. Maturilli, N. T. Mueller, D. Kappel, S. E. Smrekar, Surface weathering on Venus: Constraints from kinetic, spectroscopic, and geochemical data. *Icarus* **2020**, 114139 (2020).
42. G. Berger, A. Cathala, S. Fabre, A. Y. Borisova, A. Pages, T. Aigouy, J. Esvan, P. Pinet, Experimental exploration of volcanic rocks-atmosphere interaction under Venus surface conditions. *Icarus* **329**, 8–23 (2019).
43. H. Teffeteller, paper presented at the Lunar and Planetary Science Conference, Houston, USA, 2020 #2038.
44. I. H. Campbell, S. R. Taylor, No water, no granites—No oceans, no continents. *Geophys. Res. Lett.* **10**, 1061–1064 (1983).
45. J. Helbert, T. Sauberlich, M. D. Dyar, C. Ryan, I. Walter, J.-M. Reess, Y. Rosas-Ortiz, G. Peter, A. Maturilli, G. Arnold, The Venus Emissivity Mapper (VEM): Advanced development status and performance evaluation, paper presented at the Infrared Remote Sensing and Instrumentation XXVIII, 20 August 2020.
46. D. Kappel, R. Haus, G. Arnold, Error analysis for retrieval of Venus' IR surface emissivity from VIRTIS/VEX measurements. *Planet. Space Sci.* **113-114**, 49–65 (2015).
47. D. Kappel, MSR, a multi-spectrum retrieval technique for spatially-temporally correlated or common Venus surface and atmosphere parameters. *J. Quant. Spectros. Radiat. Trans.* **133**, 153–176 (2014).
48. A. Maturilli, J. Helbert, Characterization, testing, calibration, and validation of the Berlin emissivity database. *J. Appl. Remote Sens.* **8**, 084985 (2014).
49. R. D. Taubert, C. Monte, B. Gutschwager, J. Hartman, J. Hollandtu, Traceable calibration of radiation sources from the visible to the far infrared for space borne applications at PTB, Paper presented at the Sensors, Systems, and Next-Generation Satellites XIII, 22 September 2009.
50. A. Maturilli, J. Helbert, M. D'Amore, I. Varatharajan, Y. Rosas Ortiz, The planetary spectroscopy laboratory (PSL): Wide spectral range, wider sample temperature range, Paper presented at the Infrared Remote Sensing and Instrumentation XXVI, 18 September 2018.
51. S. Wold, H. Martens, H. Wold, The multivariate calibration problem in chemistry solved by the PLS Method, in *Matrix Pencils. Lecture Notes in Mathematics,* B. Kågström, A. Ruhe, Eds. (Springer, 1983), vol. 973.
52. C. Carey, paper presented at the Lunar and Planetary Science Conference XLVIII, Houston, USA, 2017.
53. J. A. Wegelin, *A Survey of Partial Least Squares (PLS) Methods, with Emphasis on the Two-Block Case* (University of Washington, 2000).
54. O. Korablev, A. Fedorova, J. L. Bertaux, A. V. Stepanov, A. Kiselev, Y. K. Kalinnikov, A. Y. Titov, F. Montmessin, J. P. Dubois, E. Villard, V. Sarago, D. Belyaev, A. Reberac, E. Neefs, SPICAV IR acousto-optic spectrometer experiment on Venus Express. *Planet. Space Sci.* **65**, 38–57 (2012).

Acknowledgments

Funding: This work was supported by European Union Horizon 2020 research and innovation programme under the grant agreement no. 654208 (www.europlanet-2020-ri.eu/research-infrastructure/field-and-lab-visits/ta2-distributed-planetary-simulation-facility-dpsf). G.A. was supported by a DLR-DAAD (Germany Academic Exchange Service) research grant. M.D.D. was supported by NASA grant 80NSSC18K1531 and a Helmholtz International Fellow Award. **Author contributions:** J.H. performed the analysis of the Venera 9 and 10 data using the new laboratory data. A.M. performed the high-temperature spectral measurements and calibrated the spectral data. M.D.D. provided compositions for all samples and performed the regression analysis. G.A. supported the spectral measurements. **Competing interests:** The authors declare that they have no competing interests. **Data and materials availability:** All data needed to evaluate the conclusions in the paper are present in the paper. The spectral data are available from the author on reasonable request. Additional data related to this paper may be requested from the authors.

Submitted 17 January 2020
Accepted 24 November 2020
Published 15 January 2021
10.1126/sciadv.aba9428

Citation: J. Helbert, A. Maturilli, M. D. Dyar, G. Alemanno, Deriving iron contents from past and future Venus surface spectra with new high-temperature laboratory emissivity data. *Sci. Adv.* **7**, eaba9428 (2021).